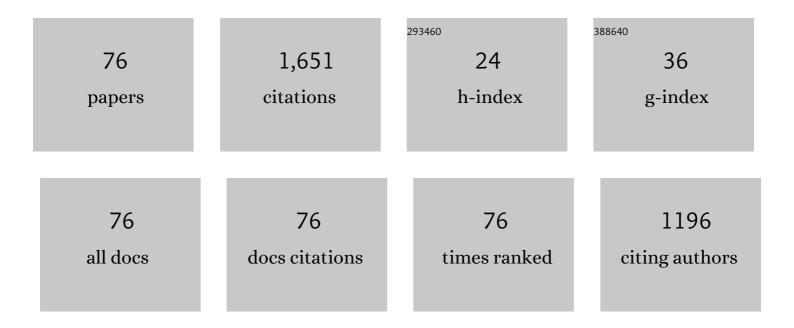
List of Publications by Year in descending order

Source: https://exaly.com/author-pdf/2444316/publications.pdf Version: 2024-02-01



#	Article	IF	CITATIONS
1	Dayâ€Toâ€Day Variability of the MLT DE3 Using Joint Analysis on Observations From TIDIâ€TIMED and a Meteor Radar Meridian Chain. Journal of Geophysical Research D: Atmospheres, 2022, 127, .	1.2	3
2	Daytime Ionospheric Largeâ€Scale Plasma Density Depletion Structures Detected at Low Latitudes Under Relatively Quiet Geomagnetic Conditions. Journal of Geophysical Research: Space Physics, 2022, 127, .	0.8	5
3	Design of Meteor and Ionospheric Irregularity Observation System and First Results. Journal of Geophysical Research: Space Physics, 2022, 127, .	0.8	8
4	Unseasonal super ionospheric plasma bubble and scintillations seeded by the 2022 Tonga Volcano Eruption related perturbations. Journal of Space Weather and Space Climate, 2022, 12, 25.	1.1	14
5	Climatology of equatorial and low-latitude F region kilometer-scale irregularities over the meridian circle around 120°E/60°W. GPS Solutions, 2021, 25, 1.	2.2	7
6	Morphological Characteristics of Thousandâ€Kilometerâ€5cale E <sub>s</sub> Structures Over China. Journal of Geophysical Research: Space Physics, 2021, 126, e2020JA028712.	0.8	15
7	Latitudinal Variations of Daytime Periodic Ionospheric Disturbances From Beidou GEO TEC Observations Over China. Journal of Geophysical Research: Space Physics, 2021, 126, e2020JA028809.	0.8	7
8	MIOS optical subsystem for determining physical and chemical properties of meteors producing plasma irregularities. Advances in Space Research, 2021, 68, 1556-1567.	1.2	5
9	The Ionosphere at Middle and Low Latitudes Under Geomagnetic Quiet Time of December 2019. Journal of Geophysical Research: Space Physics, 2021, 126, e2020JA028964.	0.8	8
10	Occurrence and Variations of Middle and Low Latitude Sporadic E Layer Investigated With Longitudinal and Latitudinal Chains of Ionosondes. Space Weather, 2021, 19, e2021SW002942.	1.3	8
11	The Prediction of Dayâ€ŧoâ€Đay Occurrence of Low Latitude Ionospheric Strong Scintillation Using Gradient Boosting Algorithm. Space Weather, 2021, 19, e2021SW002884.	1.3	9
12	Estimation of Ionospheric Total Electron Content From a Multi-GNSS Station in China. IEEE Transactions on Geoscience and Remote Sensing, 2020, 58, 852-860.	2.7	10
13	IONISE: An Ionospheric Observational Network for Irregularity and Scintillation in East and Southeast Asia. Journal of Geophysical Research: Space Physics, 2020, 125, e2020JA028055.	0.8	26
14	Observing System Impact on Ionospheric Specification Over China Using EnKF Assimilation. Space Weather, 2020, 18, e2020SW002527.	1.3	8
15	The Evolution of Complex E s Observed by Multi Instruments Over Low‣atitude China. Journal of Geophysical Research: Space Physics, 2020, 125, e2019JA027656.	0.8	8
16	Statistical Characteristics and Correlation of Low‣atitude F Region Bottomâ€Type Irregularity Layers and Plasma Plumes Over Sanya. Journal of Geophysical Research: Space Physics, 2020, 125, e2020JA027855.	0.8	12
17	Unexpected High Occurrence of Daytime Fâ€Region Backscatter Plume Structures Over Low Latitude Sanya and Their Possible Origin. Geophysical Research Letters, 2020, 47, e2020GL090517.	1.5	13
18	Persistence of the Longâ€Ðuration Daytime TEC Enhancements at Different Longitudinal Sectors During the August 2018 Geomagnetic Storm. Journal of Geophysical Research: Space Physics, 2020, 125, e2020JA028238.	0.8	15

#	Article	IF	CITATIONS
19	Interaction Between a Southwestward Propagating MSTID and a Poleward Moving WSAâ€Like Plasma Patch on a Magnetically Quiet Night at Midlatitude China Region. Journal of Geophysical Research: Space Physics, 2020, 125, e2020JA028085.	0.8	7
20	Structures of Multiple Largeâ€6cale Traveling Ionospheric Disturbances Observed by Dense Global Navigation Satellite System Networks in China. Journal of Geophysical Research: Space Physics, 2020, 125, e2019JA027032.	0.8	9
21	Deep-learning for ionogram automatic scaling. Advances in Space Research, 2020, 66, 942-950.	1.2	13
22	Low Latitude Ionospheric TEC Oscillations Associated With Periodic Changes in IMF Bz Polarity. Geophysical Research Letters, 2019, 46, 9379-9387.	1.5	26
23	The possibility of using all-sky meteor radar to observe ionospheric E-region field-aligned irregularities. Science China Technological Sciences, 2019, 62, 1431-1437.	2.0	11
24	Midlatitudinal Special Airglow Structures Generated by the Interaction Between Propagating Medium‣cale Traveling Ionospheric Disturbance and Nighttime Plasma Density Enhancement at Magnetically Quiet Time. Geophysical Research Letters, 2019, 46, 1158-1167.	1.5	12
25	The global climatology of the intensity of the ionospheric sporadic <i>E</i> layer. Atmospheric Chemistry and Physics, 2019, 19, 4139-4151.	1.9	51
26	The intensification of metallic layered phenomena above thunderstorms through the modulation of atmospheric tides. Scientific Reports, 2019, 9, 17907.	1.6	10
27	Strong Sporadic <i>E</i> Occurrence Detected by Groundâ€Based GNSS. Journal of Geophysical Research: Space Physics, 2018, 123, 3050-3062.	0.8	15
28	Was Magnetic Storm the Only Driver of the Longâ€Duration Enhancements of Daytime Total Electron Content in the Asianâ€Australian Sector Between 7 and 12 September 2017?. Journal of Geophysical Research: Space Physics, 2018, 123, 3217-3232.	0.8	87
29	Two Day Wave Traveling Westward With Wave Number 1 During the Sudden Stratospheric Warming in January 2017. Journal of Geophysical Research: Space Physics, 2018, 123, 3005-3013.	0.8	19
30	lonospheric Trend Over Wuhan During 1947–2017: Comparison Between Simulation and Observation. Journal of Geophysical Research: Space Physics, 2018, 123, 1396-1409.	0.8	15
31	Daytime F-region irregularity triggered by rocket-induced ionospheric hole over low latitude. Progress in Earth and Planetary Science, 2018, 5, .	1.1	14
32	Large cale Structure of Subauroral Polarization Streams During the Main Phase of a Severe Geomagnetic Storm. Journal of Geophysical Research: Space Physics, 2018, 123, 2964-2973.	0.8	18
33	Statistical Study on the Occurrences of Postsunset Ionospheric E , Valley, and F Region Irregularities and Their Correlations Over Lowâ€Latitude Sanya. Journal of Geophysical Research: Space Physics, 2018, 123, 9873-9880.	0.8	5
34	Observation of Shortâ€Period Ionospheric Disturbances Using a Portable Digital Ionosonde at Sanya. Radio Science, 2018, 53, 1521-1532.	0.8	13
35	New Approach to Estimate Tidal Climatology From Ground―and Spaceâ€Based Observations. Journal of Geophysical Research: Space Physics, 2018, 123, 5087-5101.	0.8	14
36	Mesospheric temperatures estimated from the meteor radar observations at Mohe, China. Journal of Geophysical Research: Space Physics, 2017, 122, 2249-2259.	0.8	21

#	Article	IF	CITATIONS
37	Regional differences of the ionospheric response to the July 2012 geomagnetic storm. Journal of Geophysical Research: Space Physics, 2017, 122, 4654-4668.	0.8	23
38	lonospheric response following the <i>M</i> <sub><i>w</i></sub> 7.8 Gorkha earthquake on 25 April 2015. Journal of Geophysical Research: Space Physics, 2017, 122, 6495-6507.	0.8	17
39	Global tidal mapping from observations of a radar campaign. Advances in Space Research, 2017, 60, 130-143.	1.2	4
40	Variations of the meteor echo heights at Beijing and Mohe, China. Journal of Geophysical Research: Space Physics, 2017, 122, 1117-1127.	0.8	16
41	Response of the equatorial and low-latitude ionosphere over the West Pacific Ocean Sector to an X1.2 solar flare on 15 May 2013. Advances in Space Research, 2017, 60, 1029-1038.	1.2	7
42	Development of the Beidou Ionospheric Observation Network in China for space weather monitoring. Space Weather, 2017, 15, 974-984.	1.3	31
43	Comparison of the ionospheric F2 peak height between ionosonde measurements and IRI2016 predictions over China. Advances in Space Research, 2017, 60, 1524-1531.	1.2	22
44	GPS network observation of traveling ionospheric disturbances following the Chelyabinsk meteorite blast. Annales Geophysicae, 2016, 34, 1045-1051.	0.6	2
45	Mapping the conjugate and corotating stormâ€enhanced density during 17 March 2013 storm through data assimilation. Journal of Geophysical Research: Space Physics, 2016, 121, 12,202.	0.8	24
46	Longâ€lasting negative ionospheric storm effects in low and middle latitudes during the recovery phase of the 17 March 2013 geomagnetic storm. Journal of Geophysical Research: Space Physics, 2016, 121, 9234-9249.	0.8	49
47	Effects of disturbed electric fields in the lowâ€latitude and equatorial ionosphere during the 2015 St. Patrick's Day storm. Journal of Geophysical Research: Space Physics, 2016, 121, 9111-9126.	0.8	60
48	Contrasting behavior of the F 2 peak and the topside ionosphere in response to the 2 October 2013 geomagnetic storm. Journal of Geophysical Research: Space Physics, 2016, 121, 10,549-10,563.	0.8	20
49	Onset location of scintillation-producing spread-F plume over Sanya. Science China Earth Sciences, 2016, 59, 1692-1699.	2.3	2
50	Investigation of ionospheric TEC over China based on GNSS data. Advances in Space Research, 2016, 58, 867-877.	1.2	26
51	Evidence for lightningâ€associated enhancement of the ionospheric sporadic <i>E</i> layer dependent on lightning stroke energy. Journal of Geophysical Research: Space Physics, 2015, 120, 9202-9212.	0.8	23
52	Shear in the zonal drifts of 3 m irregularities inside spread <i>F</i> plumes observed over Sanya. Journal of Geophysical Research: Space Physics, 2015, 120, 8146-8154.	0.8	7
53	Seasonal variations of MLT tides revealed by a meteor radar chain based on Hough mode decomposition. Journal of Geophysical Research: Space Physics, 2015, 120, 7030-7048.	0.8	25
54	Statistical characteristics of low-latitude ionospheric scintillation over China. Advances in Space Research, 2015, 55, 1356-1365.	1.2	41

#	Article	IF	CITATIONS
55	A case study of ionospheric storm effects in the Chinese sector during the October 2013 geomagnetic storm. Advances in Space Research, 2015, 56, 2030-2039.	1.2	9
56	Validation of COSMIC ionospheric peak parameters by the measurements of an ionosonde chain in China. Annales Geophysicae, 2014, 32, 1311-1319.	0.6	29
57	Interferometry observations of low-latitude E-region irregularity patches using the Sanya VHF radar. Science China Technological Sciences, 2014, 57, 1552-1561.	2.0	29
58	A statistic study of ionospheric solar flare activity indicator. Space Weather, 2014, 12, 29-40.	1.3	28
59	Comparison between ionospheric peak parameters retrieved from COSMIC measurement and ionosonde observation over Sanya. Advances in Space Research, 2014, 54, 929-938.	1.2	25
60	Observational evidence of highâ€altitude meteor trail from radar interferometer. Geophysical Research Letters, 2014, 41, 6583-6589.	1.5	7
61	A case study of postmidnight enhancement in F″ayer electron density over Sanya of China. Journal of Geophysical Research: Space Physics, 2013, 118, 4640-4648.	0.8	51
62	Tidal wind mapping from observations of a meteor radar chain in December 2011. Journal of Geophysical Research: Space Physics, 2013, 118, 2321-2332.	0.8	58
63	On the linkage of daytime 150 km echoes and abnormal intermediate layer traces over Sanya. Journal of Geophysical Research: Space Physics, 2013, 118, 7262-7267.	0.8	24
64	Precursor signatures and evolution of postâ€sunset equatorial spreadâ€F observed over Sanya. Journal of Geophysical Research, 2012, 117, .	3.3	64
65	Highâ€speed stream impacts on the equatorial ionization anomaly region during the deep solar minimum year 2008. Journal of Geophysical Research, 2012, 117, .	3.3	30
66	A comparison of lower thermospheric winds derived from range spread and specular meteor trail echoes. Journal of Geophysical Research, 2012, 117, .	3.3	18
67	A comparison of mesospheric winds measured by FPI and meteor radar located at 40N. Science China Technological Sciences, 2012, 55, 1245-1250.	2.0	25
68	Seasonal variations of night mesopause temperature in Beijing observed by SATI4. Science China Technological Sciences, 2012, 55, 1295-1301.	2.0	2
69	The first time observations of low-latitude ionospheric irregularities by VHF radar in Hainan. Science China Technological Sciences, 2012, 55, 1189-1197.	2.0	36
70	On the occurrence of postmidnight equatorial <i>F</i> region irregularities during the June solstice. Journal of Geophysical Research, 2011, 116, n/a-n/a.	3.3	56
71	Investigation of low-latitude <i>E</i> and valley region irregularities: Their relationship to equatorial plasma bubble bifurcation. Journal of Geophysical Research, 2011, 116, n/a-n/a.	3.3	25
72	Statistics of GPS ionospheric scintillation and irregularities over polar regions at solar minimum. GPS Solutions, 2010, 14, 331-341.	2.2	73

#	Article	IF	CITATIONS
73	Longitudinal development of lowâ€latitude ionospheric irregularities during the geomagnetic storms of July 2004. Journal of Geophysical Research, 2010, 115, .	3.3	44
74	GPS TEC response to the 22 July 2009 total solar eclipse in East Asia. Journal of Geophysical Research, 2010, 115, .	3.3	52
75	Observations and modeling of the ionospheric behaviors over the east Asia zone during the 22 July 2009 solar eclipse. Journal of Geophysical Research, 2010, 115, .	3.3	21
76	Occurrences of regional strong E s irregularities and corresponding scintillations characterized using a highâ€ŧemporalâ€resolution GNSS network. Journal of Geophysical Research: Space Physics, 0, , .	0.8	5